

protein antibodies, which were followed by Fluorescein (FITC)-, Rhodamine (TRITC)-, or Texas Red-conjugated anti-rat, anti-rabbit or anti-mouse antibodies, and nuclear staining (bisbenzimidazole). Samples were examined with a fluorescence or AXIOVERT 135 TV microscope (Zeiss). HeLa cells were seeded on cover glasses coated by poly-L-lysine and transfected with 2.0 µg expression plasmid DNA (pEYFP-ER, pEYFP-Mito, pEYFP; CLONTECH) using calcium phosphate precipitation. Cells were fixed in 4% paraformaldehyde, immunostained with monoclonal caspase-12 antibody and examined with a confocal microscope (Zeiss).

Generation of caspase-12 knockout mice

Gene targeting was done essentially as described¹⁷. Briefly, the caspase-12 gene fragments were cloned from a 129/sv mouse genomic library (Stratagene). DT-A fragment (pMCIDT-A; a gift from A. Yagi) was cloned into pGEM7 vector with a neomycin-resistant gene (PGK-neo). A 2.0-kilobase (kb) *SacI*-*StuI* fragment and a 9.0-kb *NotI* (cloning site from phage vector)-*XbaI* fragment were subcloned into PGK-neo-DT-A vector to generate the targeting construct. The targeting construct was transfected into J-1 ES cells by electroporation. G418 resistant transfectants were screened by genomic Southern blot analysis with a 3' flanking probe. The efficiency of homologous recombination was 5 in 232 clones. Two of the targeting clones transmitted the mutant allele. Homozygous mice were generated by interbreeding heterozygous mice (129 × C57BL/6J).

Histology and TUNEL assay of kidney and liver

Caspase-12^{+/+}, caspase-12^{+/-} and caspase-12^{-/-} littermates were injected with tunicamycin (0.25–1.0 µg g⁻¹ weight) intraperitoneally and killed 4 days after injection. Kidneys were fixed in 4% paraformaldehyde and embedded in paraffin. Histological analysis of kidney was done by haematoxylin and eosin staining. Four-week-old caspase-12^{+/+} and caspase-12^{-/-} mice were injected with Fas antibody (Jo2, 100 µg per mouse) intraperitoneally and killed 3 hours after injection. Liver and kidney were fixed in 4% paraformaldehyde and embedded in paraffin. TUNEL assay was done by manufacturers' protocols (ApopTag; Oncor).

Thymocytes culture

Thymus was dissected and passed through mesh (200–300 µm). Cells were collected by centrifugation (160g, 5 min) and resuspended in culture medium containing RPMI and 10% fetal bovine serum. Thymocytes were treated with Fas antibody (Jo2, 1 µg ml⁻¹) or dexamethasone (2 µM) for 12 hours. Percentage of cell-death was analysed by MTT (3-(4,5-dimethylthiazol-2-yl)-2,5-diphenyltetrazolium bromide; thiazolyl blue).

Embryonic fibroblast cells

Mouse embryonic fibroblast cells were prepared as described¹⁷. Briefly, homozygous caspase-12^{-/-} females mated with heterozygous males were killed at day 14.5 of gestation. Embryos were decapitated and eviscerated and carcasses were digested in trypsin. Cells were split and frozen at passage 2.

Induction of cell death

Embryonic fibroblast cells (8 × 10³ cells ml⁻¹) were treated with staurosporine (2 µM), anti-fas (Jo2, 4 µg ml⁻¹) plus CHX (10 µg ml⁻¹), or TNF (100 ng ml⁻¹) plus CHX (10 µg ml⁻¹) for 8 hours, Brefeldin A (10 µg ml⁻¹), tunicamycin (1 µg ml⁻¹) or thapsigargin (2 µM) for 24 hours. Cell death was assayed by the LIVE/DEAD viability/cytotoxicity kit.

Preparation of cell lysates and western blotting

PC12 cells treated by several drugs or serum deprivation for 36 hours were collected by scraping and lysed in lysis buffer (62.5 mM Tris-HCl pH 6.8, 2% SDS, 0.72 M β-mercaptoethanol and 7% glycerol). Lysates were analysed by western blotting using 1:50 dilution of caspase-12 antibody, 1:2500 dilution of PARP antibody, 1:10,000 dilution of tubulin antibody.

Primary cortical neuron culture and Aβ treatment

Cerebral cortex of mouse embryo at day 14.5–15.5 was freed from meninge and separated from olfactory bulb and hippocampus. Trypsinized cells were suspended in medium (DMEM/F-12, B27 (Gibco), and penicillin, streptomycin) and seeded on poly-L-lysine-coated dishes. After 4 days of culturing, neurons were incubated with either 20 µM Aβ (1–40) for 72 hours or 1.0 µM STS for 48 hours. Cell viability was determined by MTS (3-(4,5-dimethylthiazol-2-yl)-5-(3-carboxymethoxyphenyl)-2-(4-sulphenyl)-2H-tetrazolium, inner salt) assay (CellTiter 96R aqueous non-radioactive cell proliferative assay; Promega). Alternatively, apoptotic neurons were identified by characteristic nuclear morphology after fixing in 4% paraformaldehyde for 15 min at 4 °C, permeabilizing in 0.4% Triton for 10 min at room temperature and staining in Hoechst 33258 (1 µg ml⁻¹).

Antisense caspase-12 treatment

Coupling and treatment of penetratin 1 and antisense of caspase-12 were prepared as described¹⁶. Antisense caspase-12: 5'-thiol modification-TGTCCTCTGCGCCCATG GCTGT-3'-amino linker; scramble oligonucleotide: 5'-thiol modification-GTCGCTCTGTGACGCGCTGTGCTG-3'-amino linker.

Received 19 October; accepted 19 November 1999.

1. Los, M., Wesselborg, S. & Schulze-Osthoff, K. The role of caspases in development, immunity, and apoptotic signal transduction: lessons from knockout mice. *Immunity* **10**, 629–639 (1999).

2. Friedland, R. M. & Yuan, J. ICE, neuronal apoptosis and neurodegeneration. *Cell Death Differ.* **5**, 823–831 (1998).

3. Cryns, V. & Yuan, J. Proteases to die for. *Genes Dev.* **12**, 1551–1570 (1998).

4. Muzio, M. *et al.* FLICE, a novel FADD-homologous ICE/CED-3-like protease, is recruited to the CD95 (Fas/APO-1) death inducing signaling complex. *Cell* **85**, 817–827 (1996).

5. Boldin, M. P., Goncharov, T. M., Goltsev, Y. V. & Wallach, D. Involvement of MACH, a novel MORT1/FADD-interacting protease, in Fas/APO-1- and TNF receptor-induced cell death. *Cell* **85**, 803–815 (1996).

6. Li, P. *et al.* Cytochrome c and dATP-dependent formation of Apaf-1/caspase-9 complex initiates an apoptotic protease cascade. *Cell* **91**, 479–489 (1997).

7. Welihinda, A. A., Tirasophon, W. & Kaufman, R. J. The cellular response to protein misfolding in the endoplasmic reticulum. *Gene Expr.* **7**, 293–300 (1999).

8. Van de Craen, M. *et al.* Characterization of seven murine caspase family members. *FEBS Lett* **403**, 61–69 (1997).

9. Kozutsumi, Y., Segal, M., Normington, K., Gething, M. J. & Sambrook, J. The presence of misfolded proteins in the endoplasmic reticulum signals the induction of glucose-regulated proteins. *Nature* **332**, 462–464 (1988).

10. Walter, J. *et al.* The Alzheimer's disease-associated presenilins are differentially phosphorylated proteins located predominantly within the endoplasmic reticulum. *Mol. Med.* **2**, 673–691 (1996).

11. Gabuzda, D., Busciglio, J., Chen, L. B., Matsudaira, P. & Yankner, B. A. Inhibition of energy metabolism alters the processing of amyloid precursor protein and induces a potentially amyloidogenic derivative. *J. Biol. Chem.* **269**, 13623–13628 (1994).

12. Zinszner, H. *et al.* CHOP is implicated in programmed cell death in response to impaired function of the endoplasmic reticulum. *Gene Dev.* **12**, 982–995 (1998).

13. Yankner, B. A., Duffy, L. K. & Kirschner, D. A. Neurotrophic and neurotoxic effects of amyloid beta protein: reversal by tachykinin neuropeptides. *Science* **250**, 279–282 (1990).

14. Yan, S. D. *et al.* An intracellular protein that binds amyloid-beta peptide and mediates neurotoxicity in Alzheimer's disease. *Nature* **389**, 689–695 (1997).

15. Wang, S. *et al.* Murine caspase-11, an ICE interacting protease, is essential for the activation of ICE. *Cell* **92**, 501–509 (1998).

16. Troy, C. M., Derosi, D., Prochiantz, A., Greene, L. A. & Shelanski, M. L. Downregulation of Cu/Zn superoxide dismutase leads to cell death via the nitric oxide-peroxynitrite pathway. *J. Neurosci.* **16**, 253–261 (1996).

17. Matsumoto, M. *et al.* Ataxia and epileptic seizures in mice lacking type I inositol 1,4,5-trisphosphate receptor. *Nature* **379**, 168–171 (1996).

Acknowledgements

We thank Y.-k. Jung and B. Hyman for helpful suggestions; A. Yagi for pMCIDT-A; T. Noda for PGK-neo plasmids; J. L. Goldstein for anti-caspase-3; T. Rapoport for anti-TRAP; S. Nagata for W4 cells; M. Yuan for technical help in the preparation of Aβ, and S.-J. Kang for providing caspase-11 mutant mice. This work was supported in part by grants from Hoechst-Marion-Roussel and Harvard Medical School project (to J.Y.) and from Human Frontier Science Program Organization and TOYOBIO Biotechnology Foundation (to T.N.).

Correspondence and requests for materials should be addressed to J.Y. (e-mail: jyuan@hms.harvard.edu).

Anti-inflammatory cyclopentenone prostaglandins are direct inhibitors of IκB kinase

Antonio Rossi*†, Pankaj Kapahi†‡, Gioacchino Natoli†‡, Takayuki Takahashi‡, Yi Chen‡, Michael Karin†‡ & M. Gabriella Santoro*†§

* *Institute of Experimental Medicine, Italian National Council of Research, and § Laboratory of Virology, Department of Biology, University of Rome Tor Vergata, 00133 Rome, Italy*

‡ *Laboratory of Gene Regulation and Signal Transduction, Department of Pharmacology, University of California San Diego, 9500 Gilman Drive, La Jolla, California 92093-0636, USA*

† *These authors contributed equally to this work*

NF-κB is a critical activator of genes involved in inflammation and immunity^{1,2}. Pro-inflammatory cytokines activate the IκB kinase (IKK) complex that phosphorylates the NF-κB inhibitors, triggering their conjugation with ubiquitin and subsequent degradation^{3,4}. Freed NF-κB dimers translocate to the nucleus and induce target genes, including the one for cyclo-oxygenase 2 (COX2), which catalyses the synthesis of pro-inflammatory prostaglandins, in particular PGE^{5,6}. At late stages of inflammatory episodes, how-

ever, COX2 directs the synthesis of anti-inflammatory cyclopentenone prostaglandins, suggesting a role for these molecules in the resolution of inflammation⁷. Cyclopentenone prostaglandins have been suggested to exert anti-inflammatory activity through the activation of peroxisome proliferator-activated receptor- γ (refs 8, 9). Here we demonstrate a novel mechanism of anti-inflammatory activity which is based on the direct inhibition and modification of the IKK β subunit of IKK. As IKK β is responsible for the activation of NF- κ B by pro-inflammatory stimuli^{10,11}, our findings explain how cyclopentenone prostaglandins function and can be used to improve the utility of COX2 inhibitors.

Cyclopentenone prostaglandins (cyPGs) have anti-inflammatory⁷ and antiviral activity^{12,13}, and inhibit NF- κ B activation in human cells stimulated with tumour necrosis factor- α (TNF α) or 12-*O*-tetradecanoylphorbol-13-acetate (TPA) by preventing phosphorylation and degradation of the NF- κ B inhibitor I κ B α ¹⁴. I κ B α is phosphorylated by the IKK complex, which contains two catalytic subunits (IKK α and IKK β) and the IKK γ or NEMO regulatory subunit^{15,16}, at sites that trigger its ubiquitin-dependent degradation^{3,4}.

To determine whether IKK could be the target for cyPGs, we treated human lymphoblastoid Jurkat cells with the cyPG prostaglandin A₁ (PGA₁) and stimulated them with either TNF α (Fig. 1a) or TPA (Fig. 1b). Both TNF α and TPA rapidly stimulated IKK activity, which reached a maximum after 10–15 min. PGA₁ inhibited IKK activity and prevented I κ B α degradation and NF- κ B

activation by both inducers (Fig. 1a, b), but did not inhibit activation of *c*-Jun amino-terminal kinases (JNK) and p38 mitogen-activated protein (MAP) kinases (Fig. 1c). Hence, PGA₁ targets a selected subset of kinases that activate transcription factors. In addition, PGA₁ did not inhibit the DNA binding of transcription factors Oct-1 and Sp-1 (Fig. 1a). A 15-min exposure to PGA₁ was sufficient to partially inhibit IKK activity, but more substantial inhibition required longer pre-incubation (Fig. 1d). Similarly, PGA₁ inhibited IKK activity and prevented NF- κ B activation in HeLa cells stimulated with interleukin1 (IL-1) or TNF α (Fig. 1e). Thus, the inhibitory effect of PGA₁ is independent of type of cell and stimulus. However, the half-maximal inhibitory (IC₅₀) concentration of PGA₁ towards NF- κ B was 12 μ M in Jurkat cells, whereas the IC₅₀ was 65 μ M in HeLa cells (data not shown).

IKK can be activated by the overexpression of protein kinases MEKK1 (MAP kinase Erk kinase kinase 1) or NIK (NF- κ B-inducing kinase)¹⁷. When added 10 min or 18 h after the transfection of COS cells with X-press-tagged NIK, PGA₁ inhibited activation of endogenous IKK activity (Fig. 2a). In a second experiment, COS cells were co-transfected with haemagglutinin A(HA)-tagged IKK α together with either 'empty' or NIK vectors. In the conditions that we used, HA-IKK α is incorporated into functional cytokine-responsive complexes with relative molecular mass (*M*_r) 900K¹⁵. NIK-induced IKK activity was inhibited by PGA₁ added immediately after or 18 h after transfection (Fig. 2b). PGA₁

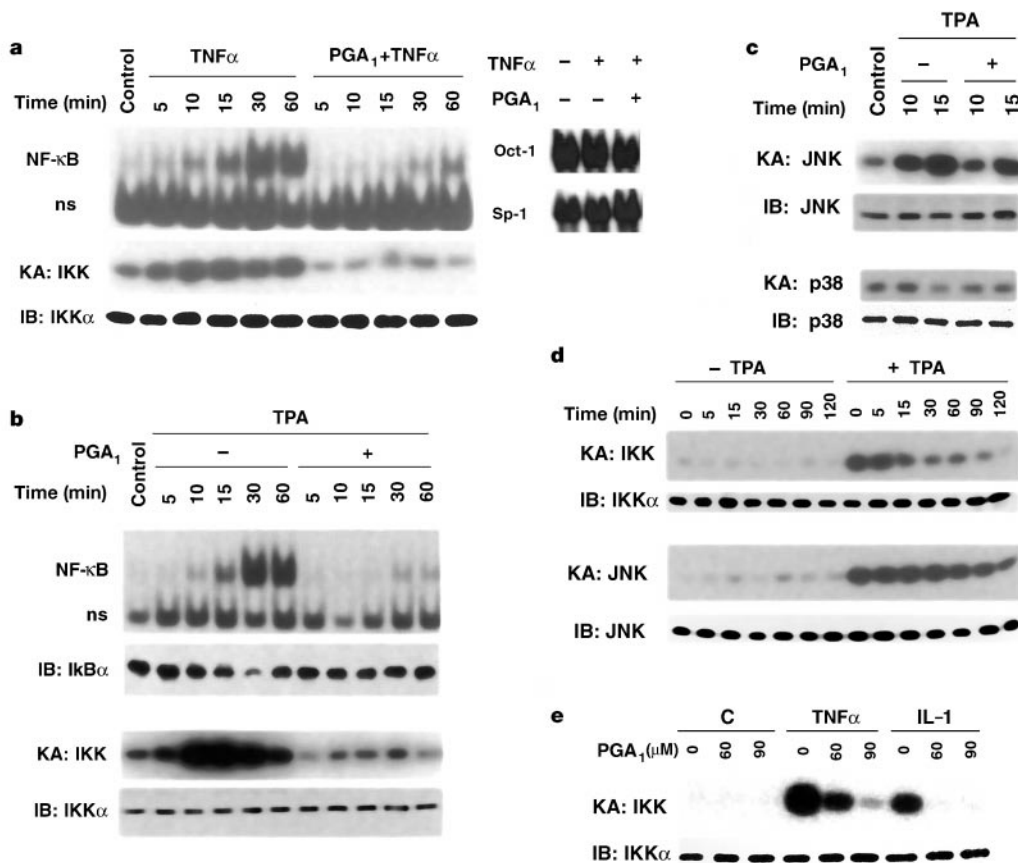


Figure 1 PGA₁ inhibits TNF α - and TPA-induced IKK and NF- κ B activities. **a**, Jurkat cells treated with 24 μ M PGA₁ or diluent for 2 h were stimulated with TNF α . At the indicated times cell lysates were prepared and assayed for NF- κ B activation by EMSA (top panel) and IKK activity by kinase assay (KA, middle panel). Positions of NF- κ B–DNA (NF- κ B) and a nonspecific protein–DNA (ns) complexes are indicated. IKK recovery was determined by immunoblotting (IB) for IKK α (bottom panel). No effects of PGA₁ (120 μ M) on Oct-1 and Sp-1 DNA-binding activities were observed (right). **b**, Jurkat cells treated with 24 μ M PGA₁ or diluent for 2 h were stimulated with TPA for the indicated times after which lysates

were prepared and assayed for NF- κ B activation (top panel), I κ B α degradation (second panel) and endogenous IKK activity (bottom panels). **c**, Samples from **b** were analysed for JNK1 and p38 activities. Recoveries of JNK and p38 were determined by immunoblotting. **d**, Jurkat cells pretreated with 24 μ M PGA₁ for the indicated times were stimulated for 15 min with TPA. Endogenous IKK and JNK activities and recoveries were determined. **e**, HeLa cells pretreated with PGA₁ were left untreated (C) or stimulated for 10 min with TNF α or IL-1. Cell lysates were assayed for endogenous IKK activity and recovery.

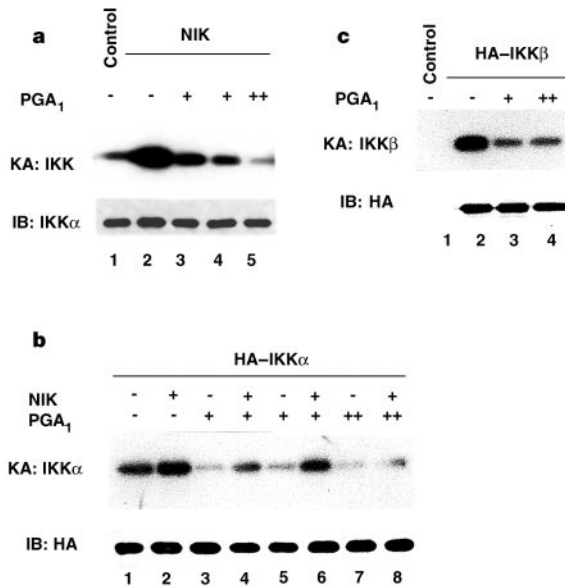


Figure 2 PGA₁ prevents NIK-induced IKK activation and inhibits IKK β activity. **a**, COS cells transfected with X-press-tagged NIK (lanes 2–5) or ‘empty’ (lane 1) expression vectors were treated with PGA₁ (15 μ M in lanes 3 and 4; 30 μ M in lane 5; either 10 min (lane 3) or 18 h (lanes 4 and 5) after transfection. Cells were lysed and assayed for endogenous IKK activity and recovery 24 h after transfection. **b**, COS cells co-transfected with HA-tagged IKK α together with ‘empty’ (–) or X-press-tagged NIK (+) expression vectors, and treated with PGA₁ (‘+’ lanes, 15 μ M; ‘++’ lanes, 30 μ M) 10 min (lanes 3 and 4) or 18 h (lanes 5–8) after transfection. Cells were lysed and assayed for HA-tagged IKK α -associated kinase activity and recovery 24 h after transfection. **c**, COS cells were transfected with empty (control, lane 1) or HA-tagged IKK β (lanes 2–4) vectors and treated with PGA₁ (‘+’ lanes, 15 μ M; ‘++’ lanes, 30 μ M) 18 h after transfection. Cells were lysed and assayed for HA-tagged IKK β kinase activity and recovery 24 h after transfection.

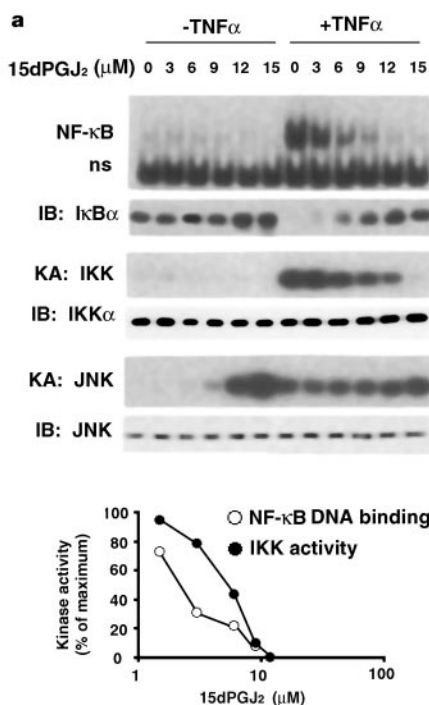
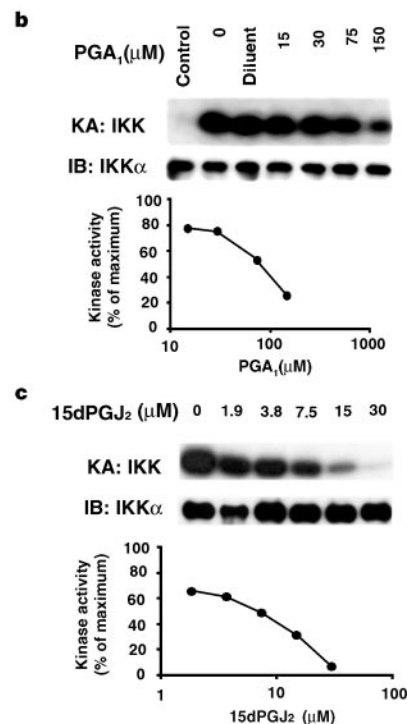


Figure 3 15dPGJ₂ inhibits IKK activity *in vivo* and *in vitro*. **a**, HeLa cells pretreated with 15dPGJ₂ for 2 h were left untreated or stimulated with TNF α for 10 min. Extracts were assayed for NF- κ B binding activity and I κ B α degradation, and for endogenous IKK and JNK1 activities (KA) and recoveries (IB). NF- κ B and IKK activities were quantified by phosphoimaging and expressed as percentage of the maximal activity achieved in the

also inhibited MEKK1-induced IKK activity in Jurkat and in COS cells (data not shown). Of the two catalytic subunits, IKK β has the major role in responding to pro-inflammatory stimuli^{10,11} and is also inhibited by high concentrations of the anti-inflammatory drug aspirin¹⁸. To determine the effect of cyPG on IKK β activity, we generated constitutively active IKK complexes, comprising mostly IKK β homodimers⁴ by overexpression of HA-tagged IKK β , in COS cells. In these cells, PGA₁ did not affect IKK β expression, as determined by immunoblotting, whereas it strongly inhibited IKK β activity (Fig. 2c).

The bioactive cyPG 15-deoxy- Δ^{12-14} -PGJ₂ (15dPGJ₂), which is physiologically formed by dehydration and isomerization of the COX metabolite PGD₂, can activate peroxisome proliferator-activated receptor- γ (PPAR- γ), a nuclear receptor that interferes with NF- κ B transcriptional activity^{8,9}. 15dPGJ₂ inhibits the production of pro-inflammatory cytokines and inducible nitric oxide synthase (iNOS) in activated monocytes by a mechanism suggested to involve PPAR- γ ^{8,9}. An anti-inflammatory effect of endogenous and exogenous 15dPGJ₂ has been shown in carrageenin-induced pleurisy in rats, which suggests that there is a physiological anti-inflammatory role for cyPGs⁷. We found that 15dPGJ₂ is a potent inhibitor of NF- κ B activation by TPA in human cells¹⁴ that express very low levels of PPAR- γ (unpublished data). We therefore examined whether 15dPGJ₂ targets IKK. In HeLa cells, which do not express PPAR- γ ⁸, 15dPGJ₂ inhibited the induction of IKK and NF- κ B activities by TNF α (Fig. 3a): the IC₅₀ for inhibition of NF- κ B DNA-binding activity was 2.25 μ M, whereas that for IKK activity was 5.08 μ M. These concentrations are comparable to those required for inhibition of cytokine synthesis^{8,9}. Intriguingly, 15dPGJ₂ stimulated JNK activity even in the absence of TNF α (Fig. 3a). 15dPGJ₂ also inhibited TNF α -induced IKK activity in human peripheral blood monocytes, but did not inhibit the DNA-binding activities of Oct1 or Sp1 (data not shown).

CyPGs also inhibited IKK activity *in vitro*. We immunoprecipitated endogenous IKK from TNF α -stimulated HeLa cells and



absence of the inhibitor. The dose–response curves represent average results from two separate experiments. **b**, **c**, HeLa cells were stimulated with TNF α for 15 min. IKK was immunoprecipitated and incubated *in vitro* with the indicated concentrations of PGA₁ (**b**), 15dPGJ₂ (**c**) or diluent for 1 h followed by kinase assay (KA) and immunoblot (IB). Kinase activity was quantified by phosphoimaging and used for plotting the dose–response curves.

determined its kinase activity in the presence of different concentrations of PGA_1 (Fig. 3b) or 15dPGJ_2 (Fig. 3c). IKK activity was inhibited in a dose-dependent fashion by both PGA_1 and 15dPGJ_2 with IC_{50} values of $79.8 \mu\text{M}$ and $7.08 \mu\text{M}$, respectively. No significant inhibition of either p38 or JNK1 activity was observed upon *in vitro* incubation with up to $60 \mu\text{M}$ 15dPGJ_2 (data not shown).

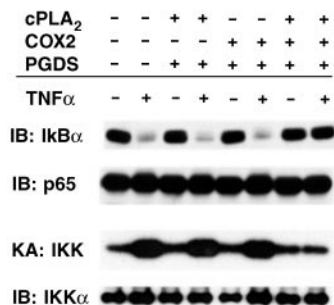


Figure 4 Inhibition of IKK activation through endogenously synthesized PGs (PGD and 15dPGJ_2). HEK 293 cells were transfected with expression vectors for cytosolic phospholipase A₂ (cPLA₂), cyclooxygenase 2 (COX2) and prostaglandin D synthase (PGDS) as indicated. After 12 h, cells were washed, incubated in low-serum (0.5%) medium for 30 h, and treated with TNF α for 15 min. I κ B α degradation and IKK activity were determined. The I κ B α immunoblot was reprobed with anti-p65 to verify equal loading of the samples.

To determine whether endogenous cyPGs are sufficient for inhibition of IKK, we transfected 293 cells with expression vectors for enzymes implicated in biosynthesis of PGD₂, which is spontaneously converted to 15dPGJ_2 by non-enzymatic dehydration^{7,19}. Combined expression of the arachidonic-acid-releasing enzyme cytosolic phospholipase A₂ (cPLA₂) with COX2 and PGD synthase (PGDS) resulted in the complete inhibition of TNF α -induced IKK activation and I κ B phosphorylation and degradation (Fig. 4). However, overexpression of each pair of enzymes (that is, cPLA₂ + PGDS and COX2 + PGDS) was insufficient for inhibition; thus, levels of cyPG that inhibit IKK can be obtained *in vivo*.

Only A- and J-type cyPGs inhibited IKK activity *in vivo* or *in vitro*; arachidonic acid and arachidonic-acid metabolites including PGB₂, PGD₂, PGE₁, PGE₂, PGF_{1 α} , thromboxane B₂ (TxB₂) and leukotriene B₄ (LTB₄) were ineffective (Fig. 5a, b). Thus, a reactive α,β -unsaturated carbonyl group in the cyclopentane ring, which renders this portion of the molecule able to form Michael adducts with cellular nucleophiles and covalently modify specific proteins^{19,20}, is essential for IKK inhibition (Fig. 5c).

The requirement for a chemically reactive cyclopentenone moiety indicated that cyPGs may inhibit IKK β through its direct modification. Many protein kinase inhibitors compete for ATP-binding sites²¹, but pre-incubation in the presence of increasing concentrations of ATP had no effect on inhibition of IKK β by 15dPGJ_2 (Fig. 6a). We also pre-incubated purified recombinant IKK β immobilized on beads with 15dPGJ_2 or diluent, and rinsed it extensively with kinase buffer lacking the inhibitor. Despite exten-

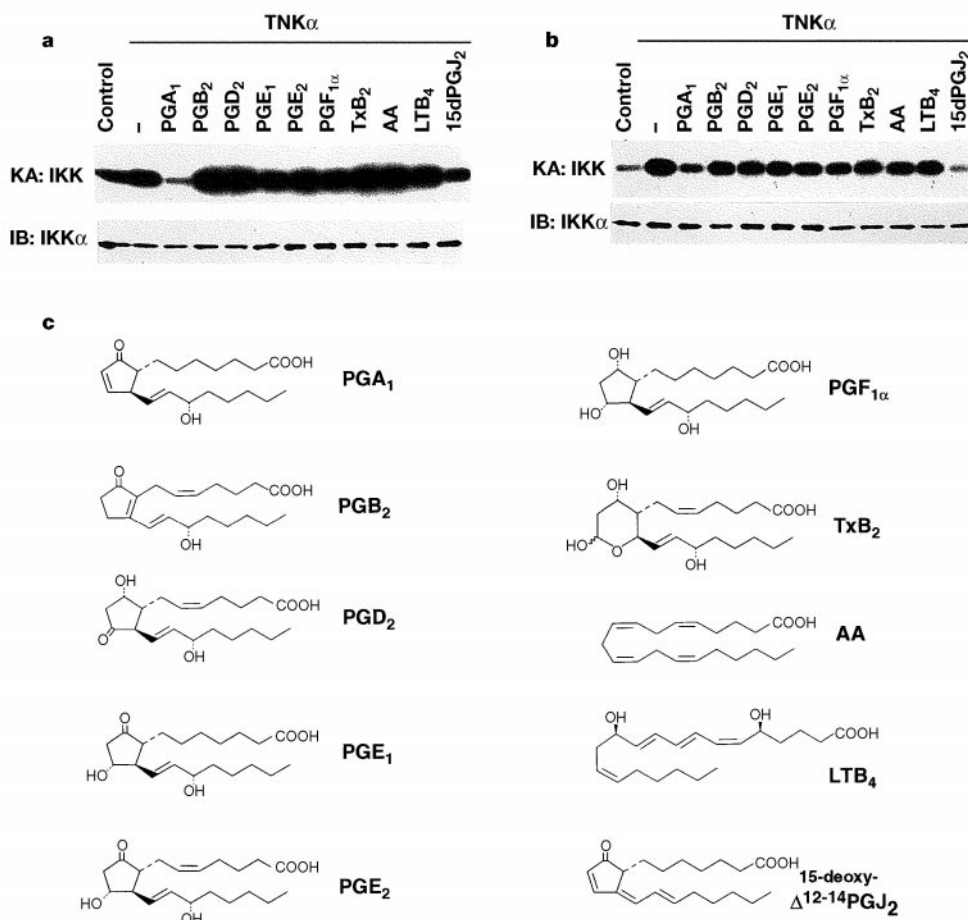


Figure 5 Effect of arachidonic acid (AA) and its metabolites on IKK activity *in vivo* and *in vitro*. **a**, HeLa cells were treated with $50 \mu\text{M}$ AA, PGA_1 , PGB_2 , PGD_2 , PGE_1 , PGE_2 , $\text{PGF}_{1\alpha}$ or TxB_2 , or $1 \mu\text{M}$ LTB_4 , or $5 \mu\text{M}$ 15dPGJ_2 for 2 h in RPMI containing 10% fetal calf serum, and stimulated with TNF α for 10 min. Cell lysates were assayed for endogenous IKK activity and recovery. Control, unstimulated cells; -, treatment with diluent alone. **b**, IKK

was immunoprecipitated from TNF α -stimulated HeLa cells and incubated *in vitro* with $100 \mu\text{M}$ AA, PGA_1 , PGB_2 , PGE_1 , PGE_2 , $\text{PGF}_{1\alpha}$ or TxB_2 or $2 \mu\text{M}$ LTB_4 or $10 \mu\text{M}$ 15dPGJ_2 followed by kinase assay and immunoblot analysis. Control, unstimulated cells; -, 1% ethanol. **c**, The structure of the different arachidonic-acid metabolites used in **a** and **b**.

sive washing, the sample that was pre-incubated with 15dPGJ₂ remained inhibited (data not shown). These results suggested that 15dPGJ₂ may inhibit IKKβ through direct modification. Plausible targets for Michael addition reactions on proteins are cysteine residues. Both IKKβ and IKKα, but not JNK1 or p38, contain a

cysteine at position 179 within their activation loop (Fig. 6b). To examine whether this cysteine is critical for sensitivity to cyPG, we replaced it with an alanine using site-directed mutagenesis. Wild-type IKKβ and IKKβ(C179A) were co-expressed with NIK in HeLa cells, and their sensitivity to 15dPGJ₂ was examined. Although both constructs were equally responsive to NIK, resulting in similar levels of kinase activity, the IKKβ(C179A) mutant was resistant to the inhibitor (Fig. 6c). Recombinant IKKβ(C179A) was also resistant to concentrations of 15dPGJ₂ that were inhibitory to wild-type IKKβ (Fig. 6d) and also to PGA₁ (data not shown). We also co-transfected an NF-κB-dependent transcriptional reporter (2XNFκB-LUC) with an expression vector encoding either wild-type IKKβ or IKKβ(C179A). A NIK expression vector was included to ensure maximal IKK activation. Whereas activation of NF-κB transcriptional activity through wild-type IKKβ was highly sensitive to 15dPGJ₂, NF-κB activation through IKKβ(C179A) was insensitive to the inhibitor (Fig. 6e). Together, these results indicate that cyPGs inhibit IKK by direct modification of its IKKβ subunit. The transfection experiments indicate that IKKβ is the critical target for cyPGs in the NF-κB activation pathway. When IKKβ is rendered resistant to modification, very little inhibition of NF-κB transcriptional activity occurs in cyPG-treated cells.

CyPGs affect cell proliferation^{19,22}, and inhibit inflammation^{7,8} and virus replication^{12,23}. Inhibition of NF-κB activation—a factor that modulates cell proliferation, differentiation and survival, controls inflammation and is required for expression and replication of certain viruses, such as HIV-1—may account for many of these effects. Although inhibition of NF-κB-mediated transcription by cyPG has been attributed to the activation of PPAR-γ, which interferes with NF-κB transcriptional activity^{8,9}, such a mechanism probably requires high levels of PPAR-γ, which are not found in many cell types. In addition, potent PPAR-γ agonists, which are not cyPGs, are poor NF-κB inhibitors^{8,24}. In particular, troglitazone, a PPAR-γ agonist, does not inhibit either IKK activity or NF-κB activation in HeLa cells stimulated with TNFα (data not shown). Here we have described a different, PPAR-γ-independent mechanism that explains the ability of cyPG to inhibit NF-κB. Prostaglandins are physiologically present in body fluids at picomolar-to-nanomolar concentrations^{19,25}; however, arachidonic-acid metabolism is highly increased in several pathological conditions, including hyperthermia, infection and inflammation^{5,6,26,27}, and local prostaglandin concentrations in the micromolar range have been detected at sites of acute inflammation²⁸. Elevated cyPG synthesis has been detected in late phases of inflammation⁸ and is associated with resolution of inflammation⁷. Therefore, concentrations of cyPG that are sufficient for IKK inhibition may occur locally during late phases of inflammatory responses. Moreover, as cyPGs probably inhibit IKK through covalent and irreversible modification, their effect could be cumulative. As COX2 synthesis is under NF-κB control^{5,6}, the inhibition of IKK by cyPGs may form a negative autoregulatory loop that contributes to resolution of inflammation. Our results suggest that cyPG and possibly more potent derivatives may have therapeutic value in the treatment of inflammatory and viral diseases, as well as certain cancers²⁹ in which inhibition of NF-κB activity may be desirable. □

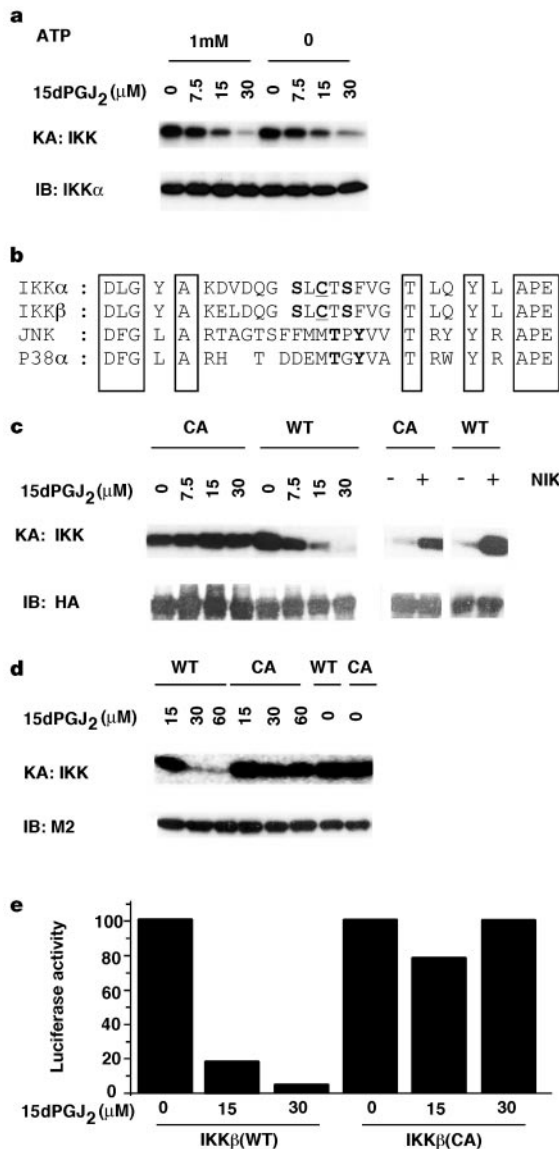


Figure 6 15dPGJ₂ is a direct inhibitor of IKKβ, whose sensitivity to inhibition is mediated by a cysteine in the activation loop. **a**, 15dPGJ₂ is not a competitive inhibitor of ATP binding. IKK was immunoprecipitated from TNFα-stimulated HeLa cells and incubated with 15dPGJ₂ (0–30 μM) with or without ATP in lysis buffer at 4 °C for 30 min. The pellets were rinsed and kinase activity measured. **b**, Sequence alignment of the activation loops of IKKα, IKKβ, JNK1 and p38α. Phospho-acceptor sites critical for kinase activation are in bold; cysteine residues of IKKα and IKKβ are underlined. **c**, HeLa cells were transiently transfected with expression vectors for wild-type IKKβ (WT) or IKKβ(C179A) (CA) with or without a NIK expression vector. After 16 h, NIK-transfected cells were treated for 2 h with 15dPGJ₂ (left panel). Kinase activity (KA) and expression (IB) were subsequently determined. **d**, Sf9 cells infected with FLAG-tagged wild-type IKKβ and IKKβ(C179A) baculoviruses were incubated with various concentrations of 15dPGJ₂ for 2 h at 28 °C, and kinase activity and expression determined. **e**, HeLa cells were transiently transfected with a 2XNF-κB-LUC reporter, a NIK expression vector and expression vectors for wild-type IKKβ (IKKβ (WT)) or IKKβ(C179A) (IKKβ (CA)). Cells were treated with 15dPGJ₂ at 3 h after transfection, and luciferase activity was determined of 24 h on duplicate samples. In each case the maximal activity achieved in the absence of inhibitor was given an arbitrary value of 100% and the other values were calculated relative to that.

Methods

Cell culture, transfection and treatments

Cells were cultured in either RPMI 1640 (Jurkat cells) or Dulbecco-modified minimum essential medium (DMEM) (HeLa or COS cells), supplemented with 10% fetal calf serum and antibiotics. Cells were stimulated with either 25 ng ml⁻¹ TPA, 20 ng ml⁻¹ recombinant human TNFα or 10 ng ml⁻¹ IL-1β (Sigma). PGA₁, 15dPGJ₂, TxB₂, LTB₄, arachidonic acid and other PGs (Cayman Chemical Co.) were dissolved in ethanol and used as described¹⁴. Controls received equal amounts of ethanol. Transfections were carried out using Lipofectamine Plus (GIBCO) for HeLa and COS cells and DEAE-dextran (Sigma) for Jurkat cells. Xpress-tagged NIK, Xpress-tagged MEKK1, HA-tagged IKKα and HA-tagged IKKβ have been described¹⁰. COX2 and cPLA₂ expression vectors (gifts from L. Feng) have been described³⁰. PGD synthase was cloned from an HT29 colon carcinoma cell line

complementary DNA library by PCR and subcloned in pCDNA3 vector. Cells were lysed in buffer B (50 mM Tris-HCl pH 7.5, 400 mM NaCl, 1 mM EDTA, 1 mM EGTA, 1% Triton, 0.5% NP-40 and 10% glycerol supplemented with 20 mM β -glycerophosphate, 19 mM PNPP, 500 mM Na₂VO₄, 1 mM PMSF, 20 μ g ml⁻¹ aprotinin, 2.5 μ g ml⁻¹ leupeptin, 8.3 μ g ml⁻¹ bestatin, 1.7 μ g ml⁻¹ pepstatin and 2 mM dithiothreitol.

Electrophoretic mobility-shift assay (EMSA)

Aliquots of total extracts (15 μ g protein) in buffer B were incubated with a ³²P-labelled NF- κ B DNA, followed by analysis of DNA-binding activity by EMSA on 4% polyacrylamide gels¹⁴. The specificity of protein-DNA complexes was verified by supershift with polyclonal antibodies specific for p65 (Rel A).

Kinase assay, immunoprecipitation and immunoblotting

Cell lysates were incubated with anti-IKK α (Pharmingen), anti-HA (12CA5; Pharmingen), anti-JNK1 (333.8; Pharmingen) or anti-p38 (New England Biolabs) for 2 h, and 15 μ l protein-A-Sepharose (Sigma) was added for 1 h. After extensive washing, kinase assays were done as described¹. Endogenous IKK, HA-tagged IKK α , HA-tagged IKK β , endogenous JNK1 and p38 activities were determined with GST-IkBa(1-54), GST-c-Jun(1-79) and GST-ATF2 as substrates. Recombinant IKK β was expressed in Sf9 cells and purified as described⁴. Arachidonic acid, PGs, LTB₄ and TxB₂ were added to washed immunoprecipitates of recombinant IKK β in kinase buffer in a final volume of 500 μ l. After 1.5 h at 4 °C, the immunoprecipitates were washed and the kinase activity was determined. Western blot analysis was done as described¹⁴.

Received 2 August; accepted 17 November 1999.

- Baldwin, A. S. The NF- κ B and I κ B proteins: new discoveries and insights. *Annu. Rev. Immunol.* **14**, 649–683 (1996).
- Barnes, P. J. & Karin, M. Nuclear factor- κ B—a pivotal transcription factor in chronic inflammatory diseases. *New Engl. J. Med.* **336**, 1066–1071 (1997).
- DiDonato, J. A., Hayakawa, M., Rothwarf, D. M., Zandi, E. & Karin, M. A cytokine-responsive I κ B kinase that activates the transcription factor NF- κ B. *Nature* **388**, 548–554 (1997).
- Zandi, E., Chen, Y. & Karin, M. Direct phosphorylation of I κ B by IKK α and IKK β : discrimination between free and NF- κ B-bound substrate. *Science* **281**, 1360–1363 (1998).
- Herschman, H. R. *et al.* Function and regulation of prostaglandin synthase-2. *Adv. Exp. Med. Biol.* **407**, 61–66 (1997).
- Newton, R., Kintert, L. M. E., Bergmann, M., Adcock, I. M. & Barnes, P. I. Evidence for involvement of NF- κ B in the transcriptional control of COX-2 gene expression by IL-1 β . *Biochem. Biophys. Res. Comm.* **237**, 28–32 (1997).
- Gilroy, D. W. *et al.* Inducible cyclooxygenase may have anti-inflammatory properties. *Nature Med.* **5**, 698–701 (1999).
- Ricote, M., Li, A. C., Willson, T. M., Kelly, C. J. & Glass, C. K. The peroxisome proliferator-activated receptor- γ is a negative regulator of macrophage activation. *Nature* **391**, 79–82 (1998).
- Jiang, C., Ting, A. T. & Seed, B. PPAR- γ agonists inhibit production of monocyte inflammatory cytokines. *Nature* **391**, 82–86 (1998).
- Delhase, M., Hayakawa, M., Chen, Y. & Karin, M. Positive and negative regulation of I κ B kinase activity through IKK β subunit phosphorylation. *Science* **284**, 309–313 (1999).
- Tanaka, M. *et al.* Embryonic lethality, liver degeneration and impaired NF- κ B activation in IKK- β deficient mice. *Immunity* **10**, 421–429 (1999).
- Santoro, M. G. Antiviral activity of cyclopentenone prostanoids. *Trends Microbiol.* **5**, 276–281 (1997).
- Rozera, C. *et al.* Inhibition of HIV-1 replication by cyclopentenone prostaglandins in acutely infected human cells. *J. Clin. Invest.* **97**, 1795–1803 (1996).
- Rossi, A., Elia, G. & Santoro, M. G. Inhibition of nuclear factor κ B by prostaglandin A₁: an effect associated with heat shock transcription factor activation. *Proc. Natl Acad. Sci. USA* **94**, 746–750 (1997).
- Rothwarf, D. M., Zandi, E., Natoli, G. & Karin, M. IKK- γ is an essential regulatory subunit of the I κ B kinase complex. *Nature* **395**, 297–300 (1998).
- Yamaoka, S. *et al.* Complementation cloning of NEMO, a component of the I κ B kinase complex essential for NF- κ B activation. *Cell* **93**, 1231–1240 (1998).
- Karin, M. & Delhase, M. JNK or IKK, AP-1 or NF- κ B, which are the targets for MEK kinase 1 action? *Proc. Natl Acad. Sci. USA* **95**, 9067–9069 (1998).
- Yin, M., Yamamoto, Y. & Gaynor, R. B. The anti-inflammatory agents aspirin and salicylate inhibit the activity of I κ B kinase- β . *Nature* **398**, 77–80 (1998).
- Fukushima, M. Prostaglandin J2-anti-tumor and anti-viral activities and the mechanisms involved. *Eicosanoids* **3**, 189–199 (1990).
- Rossi, A., Elia, G. & Santoro, M. G. 2-Cyclopenten-1-one, a new inducer of heat shock protein 70 with antiviral activity. *J. Biol. Chem.* **271**, 32192–32196 (1996).
- Gray, N. S. *et al.* Exploiting chemical libraries, structure and genomics in the search for kinase inhibitors. *Science* **281**, 533–537 (1998).
- Santoro, M. G., Garaci, E. & Amici, C. Prostaglandins with antiproliferative activity induce the synthesis of a heat shock protein in human cells. *Proc. Natl Acad. Sci. USA* **86**, 8407–8411 (1989).
- Santoro, M. G., Benedetto, A., Carruba, G., Garaci, E. & Jaffe, B. M. Prostaglandin A compounds as antiviral agents. *Science* **209**, 1032–1034 (1980).
- Stabel, B. *et al.* Activation of human aorta smooth-muscle cells is inhibited by PPAR α but not by PPAR γ activators. *Nature* **393**, 790–793 (1998).
- Serhan, C. N., Haeggström, J. Z. & Leslie, C. C. Lipid mediator networks in cell signaling: update and impact of cytokines. *FASEB J.* **10**, 1147–1158 (1996).
- Calderwood, S. K., Bornstein, B., Farnum, E. K. & Stevenson, M. A. Heat shock stimulates the release of arachidonic acid and the synthesis of prostaglandins and leukotriene B₄ in mammalian cells. *J. Cell Physiol.* **141**, 325–333 (1989).
- Leung, D. Y. *et al.* Increased *in vitro* bone resorption by monocytes in the hyper-immunoglobulin E syndrome. *J. Immunol.* **140**, 84–88 (1988).
- Offenbacher, S., Odle, B. M. & Van Dyke, T. E. The use of crevicular fluid prostaglandin E₂ levels as a predictor of periodontal attachment loss. *J. Periodontol. Res.* **21**, 101–112 (1986).

29. Wang, C. Y., Mayo, M. W. & Baldwin, A. S. TNF and cancer therapy-induced apoptosis: potentiation by inhibition of NF- κ B. *Science* **274**, 786–787 (1998).

30. Hirose, S. *et al.* Expression and localization of cyclooxygenase isoforms and cytosolic phospholipase A₂ in anti-Thy-1 glomerulonephritis. *J. Am. Soc. Nephrol.* **9**, 408–416 (1998).

Acknowledgements

We thank L. Feng for useful suggestions and for cPLA₂ and COX2 expression vectors. This work was supported by grants from the Italian Ministry of Public Health, II National AIDS Research Project (1999), the CNR Target Project on Biotechnology (G.S.), the NIH and the California Cancer Research Program (M.K.). M.K. is the Frank and Else Schilling American Cancer Society Research Professor. P.K., G.N. and Y.C. were supported by postdoctoral fellowships from the Wellcome Trust, Damon-Runyon Walter-Winchell Cancer Research Fund and the Tobacco Related Disease Research Program, respectively.

Correspondence and requests for material should be addressed to M.K. (e-mail: karinoffice@ucsd.edu).

Nuclear pore complexes in the organization of silent telomeric chromatin

Vincent Galy^{*}, Jean-Christophe Olivo-Marin[†], Harry Scherthan[‡], Valerie Doye[§], Nadia Rascalou^{*} & Ulf Nehrbass^{*}

^{*} Laboratoire de Biologie Cellulaire du Noyau, Institut Pasteur, CNRS URA 1773, 25 rue du Docteur Roux, 75724 Paris Cedex 15, France

[†] Laboratoire d'Analyse d'Images Quantitative, Institut Pasteur, CNRS URA 1947, 25 rue du Docteur Roux, 75724 Paris Cedex 15, France

[‡] Abt. Humanbiologie and Abt. Zellbiologie, der Universität, Postf. 3049, D-67653 Kaiserslautern, Germany

[§] Institut Curie, CNRS, UMR144, 22 rue Lhomond, 75248 Paris Cedex 05, France

The functional regulation of chromatin is closely related to its spatial organization within the nucleus. In yeast, perinuclear chromatin domains constitute areas of transcriptional repression^{1–3}. These 'silent' domains are defined by the presence of perinuclear telomere clusters⁴. The only protein found to be involved in the peripheral localization of telomeres is Yku70/Yku80 (ref. 5). This conserved heterodimer⁶ can bind telomeres⁷ and functions in both repair of DNA double-strand breaks^{8–11} and telomere maintenance^{7,12–15}. These findings, however, do not address the underlying structural basis of perinuclear silent domains. Here we show that nuclear-pore-complex extensions formed by the conserved TPR^{16,17} homologues Mlp1 and Mlp2^{18,19} are responsible for the structural and functional organization of perinuclear chromatin. Loss of *MLP2* results in a severe deficiency in the repair of double-strand breaks. Furthermore, double deletion of *MLP1* and *MLP2* disrupts the clustering of perinuclear telomeres and releases telomeric gene repression. These effects are probably mediated through the interaction with Yku70. Mlp2 physically tethers Yku70 to the nuclear periphery, thus forming a link between chromatin and the nuclear envelope. We show, moreover, that this structural link is docked to nuclear-pore complexes through a cleavable nucleoporin, Nup145²⁰. We propose that, through these interactions, nuclear-pore complexes organize a nuclear subdomain that is intimately involved in the regulation of chromatin metabolism.

Mlp1 and Mlp2 are putative coiled-coil proteins that are located at the interface between the nuclear envelope and the nuclear interior¹⁹. Sequence homology and similar behaviour in biochemical fractionation suggest that the two proteins have overlapping functions¹⁹. Although double mutants did not have an obvious